Nonlinear Design Procedures for Single-Frequency and Broad-Band GaAs MESFET Power Amplifiers

THOMAS J. BRAZIL AND SEAN O. SCANLAN, FELLOW, IEEE

Abstract — **The design and optimization of MESFET power amplifiers are investigated using an intermediate-level or "functional" device modeling approach. The approximations involved are discussed, together with considerations of required circuit terminations at harmonic frequencies. Three variations of the approach, based on large-signal admittance, scattering, and hybrid parameters, are compared in the design of a single-frequency amplifier, and the method is extended to broad-band power amplifier design. In all cases, results are validated by comparison with a full time-domain large-signal amplifier analysis, involving realistic, distributed external circuits.**

I. Introduction

PROCEDURES FOR the design of power amplifiers based on GaAs MESFET's are of continuing and growing interest to microwave engineers. The practical development of such amplifiers to date has relied extensively on techniques based on experimental measurements, commonly using either load-pull methods [1] or measurements of large-signal S parameters [2]. Both these approaches have their merits and difficulties. The load-pull method, for example, has the advantage of realistic test conditions; however, it is complex and time-consuming to implement. In addition, reliance on experimental data means that it is difficult to relate power amplifier performance directly to the structural and electrical parameters of the device.

In order to improve insight into large-signal behavior, a number of MESFET large-signal models have been reported in the literature (e.g. [3]–[5]). Most of these models are based on some form of nonlinear equivalent circuit, with parameters often determined using combinations of dc and small-signal measurements on the active device. Alternatively, a physical device model may be developed [6] based on a solution of the relevant carrier and field equations. The solution for a complete power amplifier requires that the device model be incorporated into an external circuit, which realistically should have a distributed character. Obtaining a full solution for such a system is a nontrivial numerical exercise, and a number of approaches have been described in the literature, often using harmonic-balance techniques [4], [7] but also using time-domain solution [6].

Manuscript received April 23, 1987; revised September 3, 1987.

The authors are with the Department of Electronic Engineering, University College Dublin, Ireland.

IEEE Log Number 8717981.

While the computer-based *analysis* of a given amplifier configuration is potentially of considerable value in amplifier development and diagnostic work, the designer would generally prefer to be able to carry out a computer-based *optimization* of the input and output external circuit. This kind of approach is now well established for broad-band or low-noise small-signal MESFET amplifier design, and well-known commercial software products are available for such applications. The difficulty in the large-signal case is that any form of accurate nonlinear amplifier solution for a realistic circuit environment is far more time consuming than the corresponding small-signal solution. Hence, standard optimization procedures requiring typically hundreds of solution runs become prohibitively costly for the large-signal case.

The purpose of this contribution is to describe an intermediate or "functional" level of device nonlinear characterization, which, while sacrificing some accuracy, is ideally suited to power amplifier optimization. Features of the present discussion include a systematic comparison of different formalisms of the intermediate level of nonlinear characterization, together with special attention to harmonic circuit termination conditions. The predictions of the design approach in both narrow-band and broad-band power amplifier applications are validated by comparison with a full numerical analysis using the original nonlinear device model and a fully distributed external circuit at both input and output.

In Section II the nonlinear device model, which is used as a vehicle to describe the design procedure, is introduced and discussed. Also, the various forms of intermediate-level circuit model are described together with their circuit implications. In Section III, the optimization of a single-frequency amplifier is presented, and the results of three variations of the design procedure are compared with each other and with independent full numerical analysis. The design of a broad-band amplifier is described in Section IV, and this is followed by conclusions in Section V.

II. Device Model and Functional Large-Signal Equivalent Circuits

While the principles of the design procedures described here are effectively independent of the type of device equivalent circuit or large-signal analysis technique em-

0018-9480/88/0200-0388$01.00

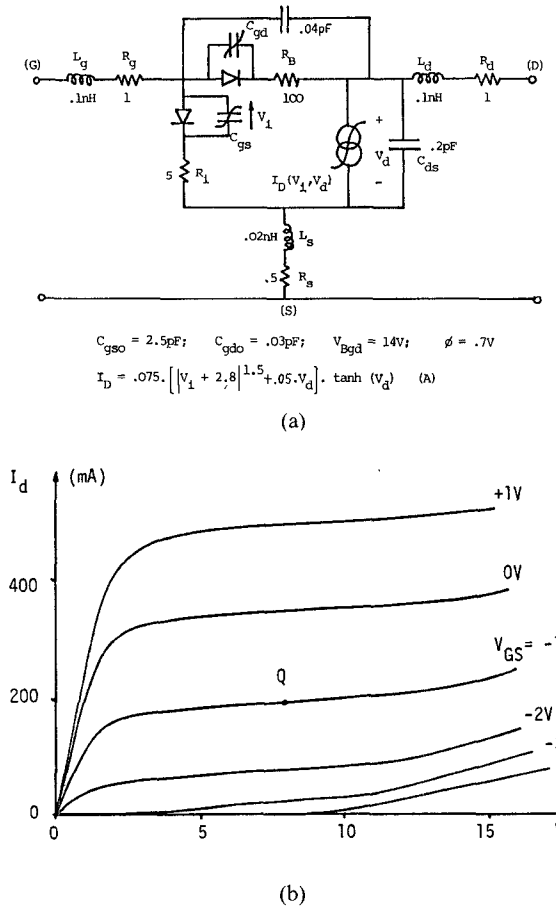

Fig. 1. (a) Nonlinear MESFET equivalent circuit. (b) DC characteristics and operating point.

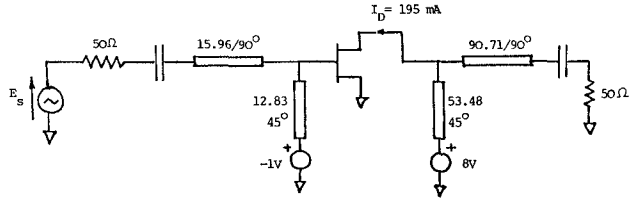

Fig. 2. Distributed matching network for maximum small-signal gain (at 10 GHz)

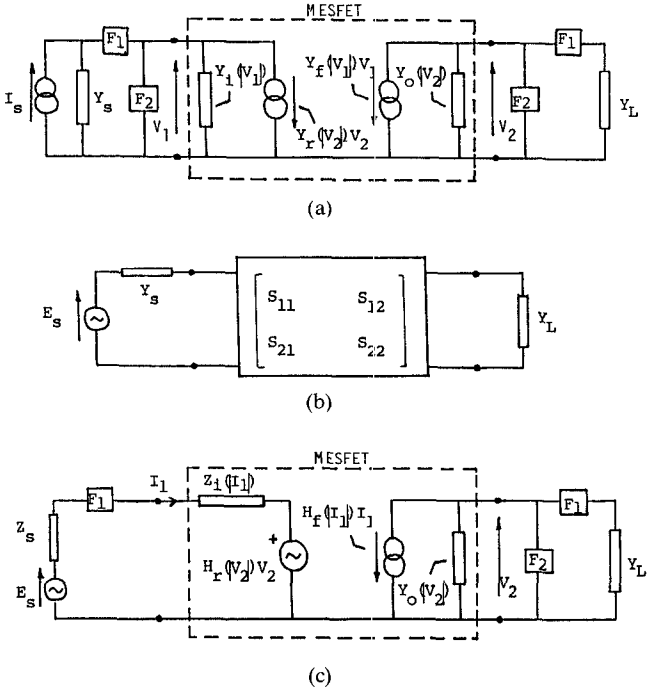

Fig. 3. Nonlinear functional equivalent circuits for MESFET. (a) Admittance model. (b) Scattering parameter model. (c) Hybrid model.

ployed, it is convenient to illustrate them with a specific example. Fig. 1(a) shows the assumed nonlinear equivalent circuit for the GaAs MESFET. This circuit incorporates the principal device nonlinearities, including voltage-dependent drain current, gate–source nonlinear capacitance, and gate–drain avalanche breakdown. The terminal drain dc characteristics are sketched in Fig. 1(b) together with the chosen (class A) bias point.

The large-signal analysis program used in the present work is a modified version of the general-purpose circuit simulator SPICE2, in which the circuit of Fig. 1(a) is built up as a subcircuit. The form of current source indicated in the model was introduced into SPICE2 by editing the source code to replace the existing level 1 MOSFET model in SPICE2 which is contained in the subroutine MOSEQ1.

A standard stability/small-signal analysis may be carried out for the device of Fig. 1, and a possible distributed matching structure to achieve the computed maximum available small-signal gain of 11.15 dB at 10 GHz is shown in Fig. 2. This network is not expected to provide maximum added-power under large-signal conditions, however, and this problem is considered further in the next section.

A central objective of the work described here is in fact to develop and evaluate functional equivalent circuits for the MESFET in order to allow optimization of large-signal operation. Three different forms of such equivalent circuits at a given frequency are indicated in Fig. 3: a large-signal admittance (Y-) model, a large-signal scattering parameter (S-) model, and a hybrid (H-) model. Other models (such as an impedance model) are possible in principle, but the three just listed have been found more convenient for MESFET devices. The elements of the models shown in Fig. 3 are, in general, complex-valued nonlinear functions of the input and output signal amplitudes at the fundamental frequency.

There are several approximations inherent in this form of large-signal modeling. In the first place, it can readily be shown that decomposition shown in Fig. 3, with elements which depend on the amplitude of one signal variable only, is not strictly valid in the nonlinear case. In addition, each model imposes specific requirements on the external circuit behavior at harmonic frequencies. For example, the Y-parameter model requires that all current harmonics be short-circuited by the external circuit. In principle, this condition may be approximated to any arbitrary degree by incorporating filters as shown in Fig. 3(a): filter F1 is ideally a short circuit at the fundamental and an open circuit at the harmonics, whereas F2 is an open circuit at

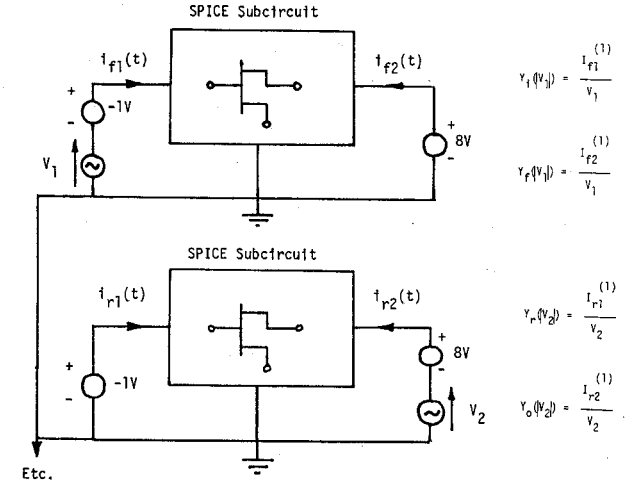

(a)

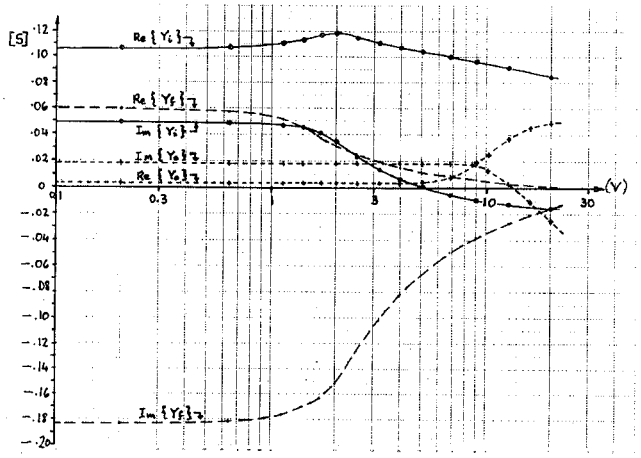

(b)

Fig. 4. (a) Circuit for evaluation of large-signal Y parameters. (b) Voltage dependence of MESFET Y parameters.

the fundamental and a short circuit at the harmonics. The large-signal S-parameter approach (Fig. 3(b)) is based on a fundamental-frequency combination of the terminal voltages and currents with $Z_S = Z_L = 50\ \Omega$. This design approach is effectively analogous to the experimental large-signal S-parameter method referred to earlier, and correct practical implementation would require that the external circuit present a matched load at the fundamental and each harmonic component of frequency.

Finally, a hybrid parameter-type model is shown in Fig. 3(c). This description requires that the external circuit at the gate appear as an open circuit at the harmonics, so that the gate current becomes sinusoidal while the gate voltage may be nonsinusoidal.

Using the nonlinear analysis program, it is quite straightforward to devise suitable embedding circuits to allow determination of the equivalent circuit parameters of Fig. 3 at a discrete number of amplitudes. Values at other drive levels may be determined subsequently by interpolation. For example, Fig. 4(a) shows a possible arrangement for Y-parameter evaluation, and Fig. 4(b) indicates the

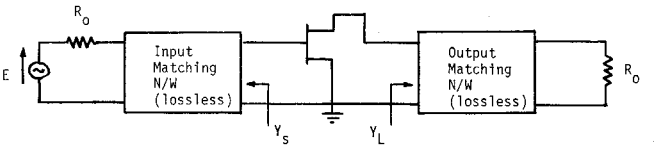

Fig. 5. MESFET power amplifier configuration.

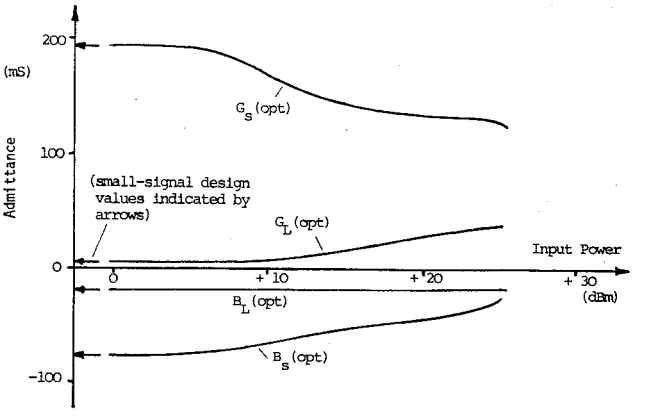

Fig. 6. Optimized source and load admittances for MESFET amplifier as a function of input drive level.

computed variation of three of the Y parameters with the terminal voltage amplitude, at a frequency of 10 GHz.

III. Optimum Design of Single-Frequency Power Amplifier

The general configuration of the single-ended amplifier considered is shown in Fig. 5, where the MESFET is the device described in Fig. 1. It is assumed that the external circuit conditions are required to achieve maximum added power at a (fundamental) frequency of 10 GHz. The optimization procedure is discussed in terms of the Y-parameter model only, since the other cases may be treated similarly. From Fig. 3(a) the following node equations may be written:

$$I_s - Y_r(|V_2|)\cdot V_2 = \left[Y_S + Y_i(|V_1|)\right]\cdot V_1 \quad (1)$$

$$-Y_f(|V_1|)\cdot V_1 = \left[Y_0(|V_2|) + Y_L\right]\cdot V_2. \quad (2)$$

A value is chosen for $V_1 (= |V_1|)$, and $|V_2|$ is then determined as a root of the nonlinear equation defined by the magnitude of (2). This allows V_2 to be found from (2) and hence I_S is obtained from (1). The gain and added power follow directly. This calculation forms the kernel of an optimization procedure involving the real and imaginary parts of Y_S and Y_L. The voltage V_1 may be stepped systematically to obtain an overall maximum added-power.

The optimized source and load admittances as a function of the input power are sketched in Fig. 6. As would be expected, the optimized values tend towards the values determined by the independent small-signal analysis and indicated by arrows on the diagram, as the input power is reduced sufficiently.

A number of plots of added-power versus input power are presented in Fig. 7. The curve labeled "small-signal

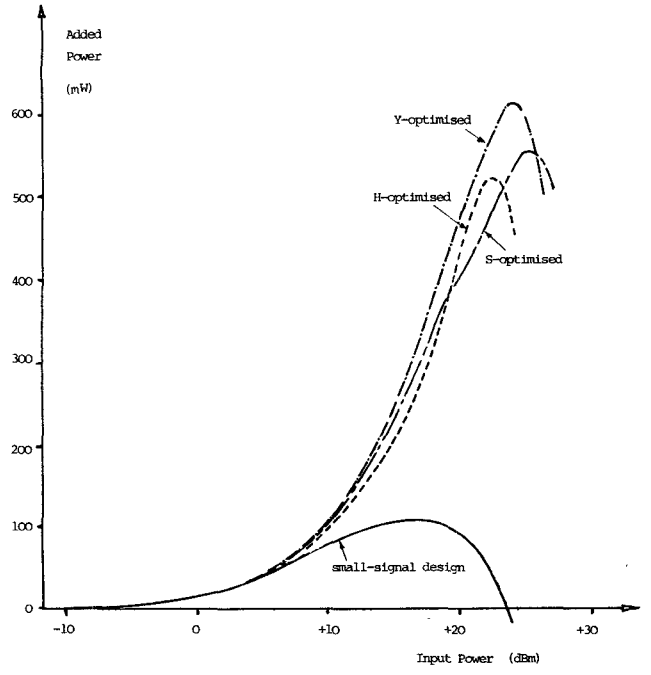

Fig. 7. Variation of amplifier added-power with input power.

TABLE I
COMPARISON OF MAXIMUM VALUES OF AMPLIFIER ADDED POWER

MODEL TYPE	OPTIMUM I/P DRIVE LEVEL	PREDICTED MAXIMUM ADDED POWER	TIME-DOMAIN SOLUTION (distributed matching circuit)	TIME-DOMAIN SOLUTION (with harmonic traps)
Y-PARAMETER	23.3 dBm	606 mW	479 mW	503 mW
S-PARAMETER	25.2 dBm	553 mW	455 mW	476 mW*
H-PARAMETER	22.2 dBm	525 mW	457 mW	493 mW

*Traps used to produce sinusoidal terminal voltages.

design" was obtained by a time-domain analysis of the circuit of Fig. 2(b), and confirms that this circuit is far from optimal for power operation. The other curves show the variation in the predicted maximum added-power using optimization procedures based on the *Y*-parameter, *S*-parameter, and *H*-parameter modeling approaches. Overall, there is fairly good mutual agreement between the various approaches; however, some differences in detail are apparent.

In order to check the predictions of Fig. 7, the time-domain analysis program was used to simulate the device (represented now by its full equivalent circuit of Fig. 1) in a distributed circuit-matching environment chosen to realize the circuit conditions for maximum added-power generated by each model. The analysis was continued until transient effects had been eliminated, and the input and output waveforms were Fourier analyzed to check amplitudes and phases. The results for added-power are summarized in the last two columns of Table I.

Two variations on this checking procedure are adopted: in the first, a general circuit of the type shown in Fig. 2(b) is used, and the results for this case are listed in the third column of the table. The second variation involves designing a circuit which more nearly presents the circuit conditions at the harmonics required by each type of model through the inclusion of at most two simple transmission line filter elements in the external circuit. These results are shown under the last column of Table I. It is seen that there is a consistent tendency for the design predictions to overestimate the simulated added-power somewhat, although generally the agreement between the two is quite good.

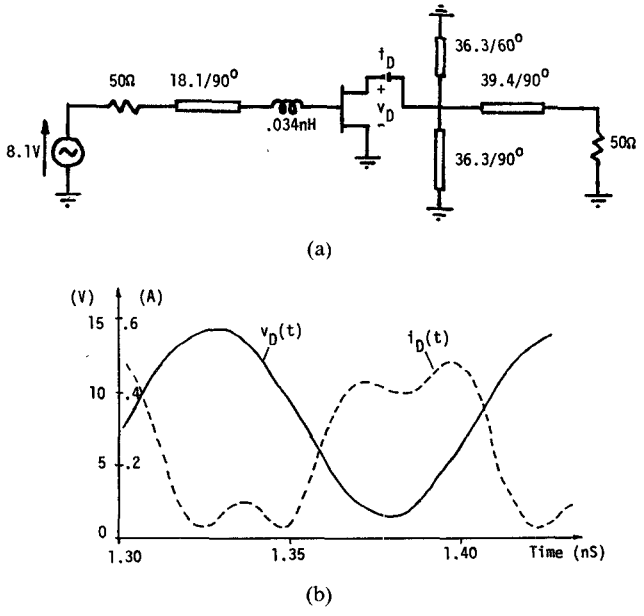

Fig. 8. (a) Circuit for maximum added power (*H*-model). (b) Drain waveforms from time-domain simulation.

TABLE II

	Fund. Comp. Gate Current	Fund. Comp. Drain Voltage	Phase	Added Power
H-Model Prediction	225 mA	6.55 V	84.7°	525 mW
Time-Domain Simulation	218 mA	6.39 V	84.8°	493 mW

While each of the three models produces broadly similar results, it is seen from Table I that for the particular case examined here, a design based on *Y* characterization provides a slightly higher added-power from the time-domain simulation than the other two models, whereas the *H* model gives best agreement between design predictions and time-domain solutions. Fig. 8(a) shows the form of external circuit used for the *H*-parameter case, where the design includes some provision for appropriate harmonic termination. The waveforms at the drain obtained from time-domain simulation are sketched in Fig. 8(b), and Table II shows good detailed correlation between the results of this simulation and the predictions of the *H*-parameter design.

IV. Optimum Design of Broad-Band Power Amplifier

The extension of the procedures described in the last section to broad-band power amplifier design is discussed here in terms of the *Y*-parameter characterization only.

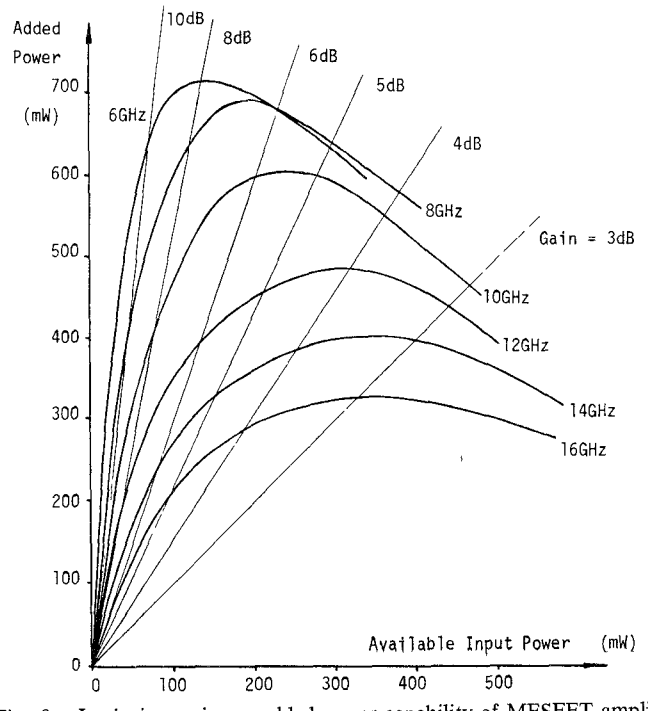

Fig. 9. Intrinsic maximum added-power capability of MESFET amplified at various frequencies.

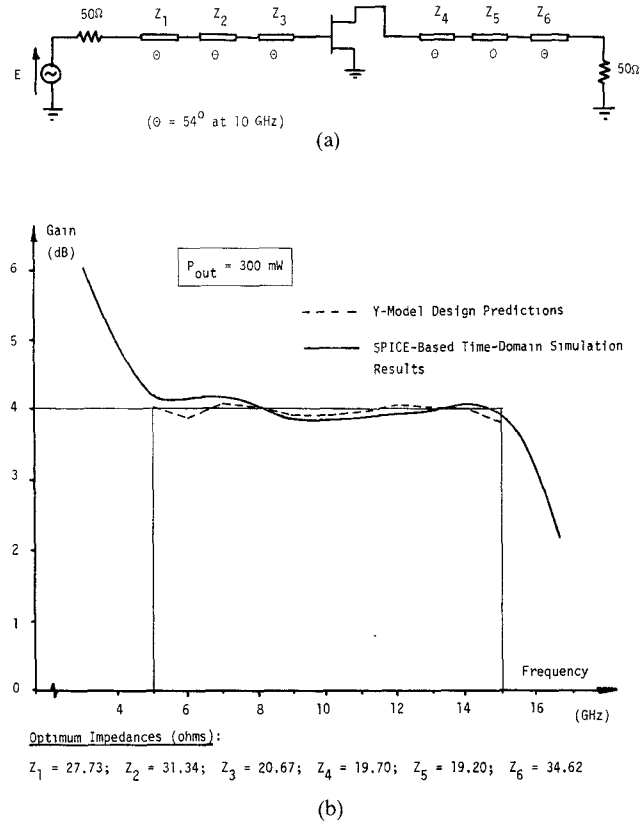

Fig. 10. (a) Example of broad-band MESFET power amplifier design. (b) Amplifier specification and results.

The other cases may be treated similarily. The Y parameters are determined at several discrete frequencies so that they become complex-valued functions of two real variables ($Y_i(f, |V_1|)$ etc.), and two-dimensional interpolation may be used for intermediate values of frequency or amplitude. Before a design specification is defined, it is useful to assess the intrinsic added-power capability of the device as a function of frequency. This information is presented as a chart in Fig. 9, where each curve represents the optimized added-power as a function of input power based on the Y-parameter characterization at a given frequency. Lines of constant gain are also shown.

Two points may be noted here. In the first place, concepts such as "gain" and "available input power" must generally be used with some care in the broad-band case; however, for the system considered here (cf. Fig. 5), where the matching networks are lossless, they effectively retain their single-frequency meaning. In the second place, a problem arises with the functional characterization when the bandwidth exceeds an octave, since, for example, the Y-parameter model applied at the lower band edge implies that the external circuit is a short circuit within the upper band edge, where the second harmonic of the lower frequency will be found. In practice, this has not been found to be a serious problem, since it is usually possible to drive the device less hard at lower frequencies than at higher frequencies to achieve a specified performance within a band. Thus, it is normally sufficient to ensure that the circuit admittance is high in the vicinity of harmonics of the upper band edge to obtain essentially sinusoidal terminal voltage across the band.

From the data in Fig. 9, it is possible to infer a realizable gain–bandwidth specification for the device. Using an optimization procedure similar to that described in the previous section, source and load admittance functions may be determined, for which a network synthesis may be attempted. Alternatively, a real frequency matching approach [8] can be used. For the example given here, a simple network topology of a cascade of three commensurate lines at input and output is chosen (see Fig. 10(a)), and the six resulting characteristic impedance values are used as optimization variables.

The specification chosen (with reference to Fig. 9) is for 4 dB of gain at 300 mW output power over the frequency range from 5 GHz to 15 GHz. The result of the Y-parameter-based optimization is shown in Fig. 10(b) as a broken line. When the optimized characteristic impedances are used in the time-domain simulator, the frequency response shown as a solid line in Fig. 10(b) is obtained, which is very close to the required behavior. A number of similar design exercises have been undertaken and checked using different power levels, gains, and bandwidths, and comparable results have been achieved in each case. The time-domain solution may also be used to check the stability of the final design, by establishing that the output power falls toward zero as the input drive is reduced.

V. Conclusions

A general approach to large-signal optimization of MESFET power amplifiers has been described and evaluated. While some sacrifice in accuracy is required and circuit conditions at harmonic frequencies must be kept

under control, very fast and flexible optimizations of narrow-band and broad-band power amplifier performance become possible. Three types of large-signal functional equivalent circuit have been investigated in a single-frequency amplifier and their design predictions compared and validated against a full time-domain analysis.

It may be noted that in principle it would be possible to augment each of the models in Fig. 3 to allow for higher harmonics; however, even including only the second harmonic would lead to a much more complex device characterization procedure, while each amplifier solution would require the solution of a series of nonlinear simultaneous equations in six unknowns. The results presented here show that a fundamental frequency model alone produces quite acceptable results.

The method has been successfully extended to broad-band power amplifier design, and may in principle be readily adapted to multistage amplifiers, balanced amplifiers, or distributed power amplifiers. The method may also serve as the basis for a MESFET oscillator design procedure [9].

REFERENCES

[1] R. S. Tucker and P. D. Bradley, "Computer-aided error correction of large-signal load-pull measurements," *IEEE Trans. Microwave Theory Tech.*, vol. MTT-32, pp. 296–300, Mar. 1984.

[2] R. S. Tucker, "RF characterization of microwave power FET's," *IEEE Trans. Microwave Theory Tech.*, vol. MTT-29, pp. 776–781, Aug. 1981.

[3] Y. Tajima, B. Wrona, and U. Mishima, "GaAs FET large-signal model and its application to circuit designs," *IEEE Trans. Electron Devices*, vol. ED-28, pp. 171–175, Feb. 1981.

[4] D. L. Peterson, A. M. Pavio, and B. Kim, "A GaAs FET model for large-signal applications," *IEEE Trans. Microwave Theory Tech.*, vol. MTT-32, pp. 276–281, Mar. 1984.

[5] Y. Tajima and P. D. Miller, "Design of broad-band power GaAs FET amplifiers," *IEEE Trans. Microwave Theory Tech.*, vol. MTT-32, pp. 261–267, Mar. 1984.

[6] A. Madjar and F. J. Rosenbaum, "A large-signal model for the GaAs MESFET," *IEEE Trans. Microwave Theory Tech.*, vol. MTT-29, pp. 781–788, Aug. 1981.

[7] A. Materka and T. Kacprzak, "Computer calculation of large-signal GaAs FET amplifier characteristics," *IEEE Trans. Microwave Theory Tech.*, vol. MTT-33, pp. 129–135, Feb. 1985.

[8] H. J. Carlin and J. J. Komiak, "A new method of broad-band equalization applied to microwave amplifiers," *IEEE Trans. Microwave Theory Tech.*, vol. MTT-27, pp. 93–99 Feb. 1979.

[9] T. J. Brazil and S. O. Scanlan, "A non-linear design and optimization procedure for GaAs MESFET oscillators," in *1987 IEEE MTT-S Int. Microwave Symp. Dig.* (Las Vegas, NV), pp. 907–910.

Thomas J. Brazil was born in Co. Offaly, Ireland, on September 4, 1952. He received the B.E. degree in electrical engineering (with first class honors) from University College Dublin in 1973 and the Ph.D. in electronic engineering from the National University of Ireland in 1977.

He worked as a research engineer at Plessey Research (Caswell) U.K. until 1979, and after a period as a lecturer at the University of Birmingham, U.K., he returned to U.C.D. in 1980 to take up his current position of lecturer in the Department of Electronic Engineering. His research interests include nonlinear microwave CAD applications, device and circuit modeling, and high-data-rate optical communications.

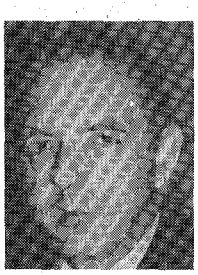

Sean O. Scanlan (M'62–SM'66–F'76) was born in Dublin, Ireland, on September 20, 1937. He received the B.E., M.E., and D.Sc. degrees from the National University of Ireland, and the Ph.D. degree from the University of Leeds, England.

From 1963 to 1973 he was with the University of Leeds, where he was Professor of Electronic Engineering from 1968. Since 1973 he has been Professor of Electronic Engineering at University College Dublin, Ireland, where his interests have been in the fields of circuit theory, communications, and solid-state devices.

Dr. Scanlan is a Fellow of the Institute of Mathematics and its applications and a Member of the Royal Irish Academy.